Performance Analysis of H-Type Vertical Axis Wind Turbine by Using Novelty Numerical Simulink Method

Muhammad Radhiva, Muhammad Hasya Abdillah, Geordiano Devanaldy Khresna Putra, Muhammad Raihan Wajdi, Putri Wulandari, Wahyu Caesarendra, Ahmad Husin Lubis, and Ary Syahriar

Abstract Renewable energy is a solution to displace non-renewable energy resources with the wind turbine being one of the prominent the renewable energy sources. Research on wind turbines still ongoing to be advanced. The Horizontal Axis Wind Turbines (HAWTs) are more widely utilized for electricity production, Vertical Axis Wind Turbines (VAWTs) offer distinct advantages not found in HAWTs. However, VAWT has several benefits that are not present in HAWT, so research on VAWT must continue with the aim that VAWT can be developed into a commercial power generator. This paper is a form of Darrieus VAWT research development. The demonstration of Numerical Simulink Method can be found here to evaluate the performance of Wind Turbine such as the values of power coefficient, angular velocity, and torque. The input parameters are a symmetrical airfoil with 15% thickness, a radius of 0.5 m, a height of 1 m, and a chord length of 0.2 m. Numerical analysis using the Novelty Simulink Model is carried out so that engineers or scientists can evaluate VAWT performance under various conditions for further research. This paper also presents a graph depicting a relationship between all output parameters with wind speeds starting from 1 m/s until 12 m/s. According to the study's outcome, these have a relation with increasing wind speed. Moreover, this research provides evidence that the VAWT can work properly at low wind speeds (less than 12 m/s).

Keywords VAWT · Start-up ramp condition · Airfoil NACA 0015 · Torque · Coefficient of power · Low wind speed

M. Radhiva · M. H. Abdillah · G. D. K. Putra · M. R. Wajdi · P. Wulandari · A. H. Lubis · A. Syahriar (✉)
Faculty of Science and Engineering, University Al-Azhar, Jakarta, Indonesia
e-mail: ary@uai.ac.id

W. Caesarendra
Faculty of Integrated Technologies, Universiti Brunei Darussalam, Bandar Seri Begawan, Brunei

H. Malik et al. (eds.), *Renewable Power for Sustainable Growth*,
Lecture Notes in Electrical Engineering 1086,
https://doi.org/10.1007/978-981-99-6749-0_14

1 Introduction

Demand of electrical energy has increased significantly along with the increase in population and demand for industry and so on. Currently the fuel used to produce electrical energy is fossil fuels such as coal, natural gas, and oil. Fossil fuels are hydrocarbons that have an environmental impact when used. When more fossils are extracted from the earth, the great of greenhouse gases that pollute the air on earth will increase. These harmful gases produced by fossil fuels have impacts on global warming [1].

Global warming is a situation in which the Earth's temperature rises due to a multitude of factors. The increase in greenhouse gases is the most influential factor in global warming. Fossil fuel combustion sources such as transportation and non-renewable power plants are factors that cause excessive toxic gases such as CO_2, methane, nitrous oxide, and SO_2 to be produced [2]. In addition, living creatures on earth are sure to be affected, directly or indirectly, because the gases produced are very dangerous to the environment and health. In terms of the environment, the intensity of natural disasters will increase, as extreme weather occurs more frequently as a result of rising temperatures. Not only that, life in the oceans and freshwater systems is also affected. Life in the oceans and freshwater systems is affected because CO_2 can dissolve, causing a decrease in water pH. In addition, the heat from greenhouse gases is trapped and absorbed by water, causing it to heat up [3]. In terms of health, there are various diseases caused by global warming because, fundamentally, global warming contributors are not only CO_2, so it can be said to be directly proportional to air pollution. For children, the effects of air pollution include infant mortality, low birth weight, allergies, asthma, nerve development damage, disabilities, and cancer, which some of these effects can be experienced by adults [4].

The Paris Agreement, enacted in 2015, was created in response to the extensive impact of global warming. In this agreement, 197 countries concurred to limit the maximum temperature rise to no more than 2 °C [5]. This means that the use of fossil fuels is increasingly restricted, as they contribute to the production of dangerous gases and rising air temperatures, in order to keep the global surface temperature increase to only 1.5 °C, which is better than the targeted 2 °C. Oil, natural gas, and coal are therefore expected to remain unexploited, leaving only 58%, 56%, and 89% respectively by 2050 [6]. Therefore, there is a need for special attention to be given to renewable energy like wind, solar, water, biomass, and geothermal so they can be used more massively as they are more environmentally friendly, have lower usage costs, and are not exhaustible. Wind power utilization is one of many solution for reducing the use of non-renewable energy. Wind energy converted into electrical energy through a generator has been proven to produce relatively low air pollution, resulting in lower impacts on living beings and the environment. Furthermore, in terms of the economy, the benefits of adopting renewable energy steadily escalate. In the year 2015, the proportion of renewable energy attained 15%. It is predicted that by 2050, the share of renewable energy will continue to grow given the public's concerns about environmental health issues, reaching 63% of energy production revenue [7].

Nowadays, there are two common categories of wind turbines which are distinguished according to the direction of their axis, To be precise, it was the Horizontal-Axis Wind Turbine (HAWT) and the Vertical-Axis Wind Turbine (VAWT). HAWT has a shape similar to aircraft propellers, which are Aligned with the wind flow, thus requiring a special mechanism to direct the blades according to the movement of the wind. The other type is VAWT, which has its axis orthogonal to the wind flow. The advantage of VAWT is that no matter where the wind comes from, it will continue to rotate, so no special mechanism is needed to rotate its blades. Both types of turbines are still being developed in order to achieve a high level of efficiency [8].

In generating electricity from a steady wind flow with sufficient speed, HAWT is clearly superior and can produce much more energy than VAWT. Additionally, HAWT exhibits more efficient performance than VAWT [9]. HAWT is commonly used in large wind farms, remote access areas, and offshore locations where the wind speed is stable and uninterrupted. On the other hand, wind patterns in urban areas tend to be unstable with low wind speeds, unpredictable wind directions, and full of turbulence which make HAWT relatively ineffective. Therefore, VAWT can be a better choice for urban areas [10]. However, VAWT is more effective when the wind direction is constantly changing because VAWT does not require a mechanism to adjust to changing wind direction. Because of this, VAWT can be utilized in other areas such as in the middle of a highway, which can be used to power the lighting system [11]. Another advantage of VAWT is that more VAWTs can be installed on a single piece of land compared to HAWT, resulting in greater energy density for VAWT usage on that land [12].

The research uses the four-digit NACA series from the National Aeronautics and Space Administration (NASA) as an airfoil of the wind turbine. Symmetrical airfoils have better efficiency but worse self-starting ability than chambered airfoils [13]. A symmetrical airfoil called the NACA 0015, which has a thickness of 15%, was used in the experiment because it can produce a maximum power coefficient at the optimum tip speed ratio (λ) higher than 3 [14, 15]. Based on Song's simulation, it was found that NACA 0015 and 0018 are more suitable for use in VAWT. Moreover, it was also found that the torque produced by NACA 0015 is not too bad, although NACA 0018 is the best [16].

This research was conducted to determine the characteristics of a vertical axis Darrieus type wind turbine using the Simulink Numerical Method. Research related to simulation methods is necessary, as a lightweight and accurate simulation method is still being sought. So far, there are two simulation methods that are often used, namely Double Multiple Streamtube (DMST) and Computational Fluid Dynamic (CFD) [17]. Although they are simulation methods that meet the needs of VAWT simulation, research on numerical methods with Simulink is very likely to be the initial step towards eventually surpassing both methods. Another advantage of this method is that we can apply control systems and generators within it. However, in this paper, we will only review its aerodynamic performance and ensure that the model has shown correct calculations [18].

2 Research Theory

In the concept of wind turbine efficiency, it is related to the betz limit. The betz limit is the maximum efficiency value that can be achieved on a wind turbine. This concept was first introduced by a physicist from Germany named Albertz Betz in 1919. The value of the betz limit is 16/27 or 59.3%, which means that the maximum limit of wind kinetic energy that can drive a turbine is only 59.3% as shown in Fig. 1. But in fact, no wind turbine can reach the maximum limit of this betz limit. The average wind turbine efficiency value is only 35–45%. [19]

However, according to Divakaran [21] there are many studies which prove that the Betz limit does not apply to VAWT. Other research says that the Betz limit still applies with a different maximum. The maximum efficiency value that applies to VAWT is 63%. Of course, it seems impossible if the efficiency of a wind turbine is close to 100%. therefore, in this study, it is assumed that the maximum possible efficiency is 64% [22].

The power in the wind turbine is the result of the conversion of wind energy that drives the rotor and generator. The amount of power in a wind turbine is highly dependent on the speed of the wind that drives the rotor. The power equation for the wind turbine is as follows:

$$P = \frac{1}{2}\rho C_{\mathrm{p}} A V o^3 \tag{1}$$

with

$$A = Hd \tag{2}$$

where P is wind turbine power (watts), is air density (1.225 kg/m^3), C_{p} is Coefficient of Power, Vo is freestream wind speed (m/s), A is rotor area (m^2), H is the height of the wind turbine (m), and d is the diameter of the rotor (m) [23].

Coefficient of power (C_{p}) is a coefficient that determines the amount of power performance of the wind turbine. This C_{p} is basically influenced by two factors, namely the yield power of the wind turbine and the kinetic energy of the wind flow

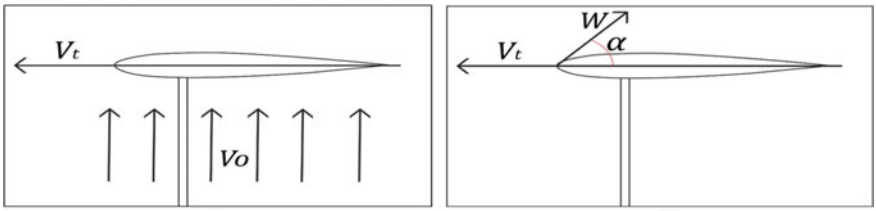

Fig. 1 **a** Illustration of freestream wind flow through the blade and **b** Illustration of relative wind flow [20]

itself. This C_p has a directly proportional relationship with the performance of the wind turbine, the greater the C_p, the better the performance of the wind turbine. The Coefficient of Power (C_p) equation is as follows:

$$C_p = \frac{Pr}{Pw} = \frac{\tau\omega}{\frac{1}{2}\rho A V o^3} \tag{3}$$

where C_p is the Coefficient of Power, Pr is the actual turbine power (Watts), and Pw is the Power of the theoretical wind speed (Watts) [19].

Tip speed ratio (λ) is one of the crucial factors in determining the design of wind turbine. λ may be defined as the ratio of wind speed with wind turbine blade tip velocity. λ is a dimensionless quantity that states the relationship between wind speed and the average rotation of the rotor [24]. The equation can be written as:

$$\lambda = \frac{\omega R}{Vo} \tag{4}$$

where λ is Tip speed ratio, ω is turbine rotor rotation speed, R is rotor radius (m), Vo is freestream windspeed (m/s) [25].

The force experienced by the blade in the direction from the trailing edge to the leading edge is the simple definition of tangential force. The tangential force can be found by the following equation:

$$F_t = C_t \frac{1}{2}\rho c h W^2 \tag{5}$$

where F_t is tangential force (N), C_t is tangential force coefficient, is air density (1.225 kg/m^3), c is cord length, h is turbine height, and W is relative wind flow.

Tangential force can be obtained from the accumulation of lift and drag forces, so that the tangential coefficient C_t is a constant value that accumulates constant values of drag and lift forces. To find the tangential force, the value C_t can be calculated with the following equation:

$$C_t = C_d \sin(\alpha) - C_l \cos(\alpha) \tag{6}$$

where C_t is tangential coefficient, C_d is coefficient drag force, C_l is coefficient lift force, and α is angle of attack.

Angle of Attack is the angle between the relative windflow (Vo) vector line and the tangential moving blade direction vector Vt. angle of attack has an effect on C_t, Therefore, the angle of attack also has a very significant effect on the torque value on the blade.

To find the angle of attack on this wind turbine, we can use the following equation:

$$\alpha = \tan^{-1}\left(\frac{\cos\theta}{\frac{\lambda}{(1-u)} + \sin\theta}\right) \tag{7}$$

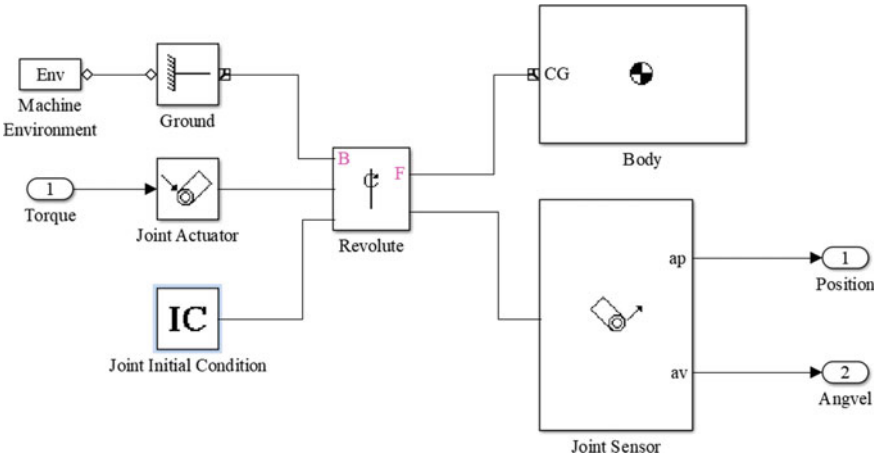

Fig. 2 Subsystem of dynamic measurement [26]

where τ is the angle of attack, u is induction factor, and θ is angular position (rad).

Relative Windflow is the wind flow in terms of the blade. Figure 1a shows freestream windflow heading towards a moving blade. While Fig. 1b shows us the direction of the wind flow when viewed from a moving blade. The value of the Relative Windspeed can be calculated by the following equation:

$$W = Vo\sqrt{[\lambda + (1-u)\sin(\theta)]^2 + [(1-u)\cos(\theta)]^2} \tag{8}$$

$$u = \frac{Nc\omega}{2\pi Vo}\sin(\theta) \tag{9}$$

where N is number of blade, c is blade chord length (m), h is height (m), W is relative wind flow, θ is angular position (rad), λ is tip speed ratio, ω is angular sepeed (rad/s), Vo is freestream windspeed (m/s), u is induction factor, and R is rotor radius (m) [27].

Torque is the value of the moment of force that states the object is rotating on its axis. Therefore, the torque value can be calculated as

$$\tau = \frac{\rho \times H \times Ct \times W^2 \times c}{2} \tag{10}$$

where is the torque (Nm), where C_t tangential force coefficient, W is relative wind speed (m/s), H is blade height (m), ρ is air density [28].

3 Methodology

Simulink is an additional part of the Matlab software that can be used as a means of modeling, simulating and analyzing dynamic systems using a graphical interface (GUI) [29]. In this study, Simulink is used to determine the value of angular velocity, torque, and power coefficient at start-up ramp condition. Matlab is also used to plot comparison charts based on parameters on Table 1. the equations that are used are applied to the Simulink that have been compiled. Finally, the angular velocity, torque, and power coefficient are shown. The parameters used in this experiment are listed in Table 1. The air pressure at the wind turbine location is assumed to be an average temperature in the world at the industrial revolution (1850) had just begun, 15 degrees Celsius, so the air density equal to 1.225 kg/m^3 [30]. The minimum wind speed used is 1 m/s and the maximum is 12 m/s. The rest of the specifications of the VAWT will be determined based on the results of this test. Table 1 is a lists of the parameters.

To calculate the angular velocity and angular position of the VAWT that being analyzed, the block set from Woods [26] will be used, as shown in Fig. 2. This subsystem block describes how the 3D shape of the turbine is used to calculate a rotational object using momentum theory. The sensor will calculates the VAWT and displays it to the user in the form of numbers.

Still based on Woods' presentation, it has been explained that a coefficient called a Simple Model Generator exists. During the experiment, it was found that this Simple

Table 1 Parameters of VAWT simulation

Parameters	Value
Air density	1.225 kg/m^3
Reynold number	80,000
Wind velocity	1 – 12 m/s
Blade number	3
Radius	0.5 m
Height	1 m
Airfoil	NACA 0015
Chord length	0.2 m

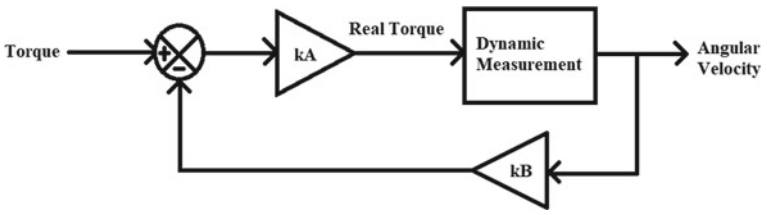

Fig. 3 System for finding a real torque and angular velocity [26]

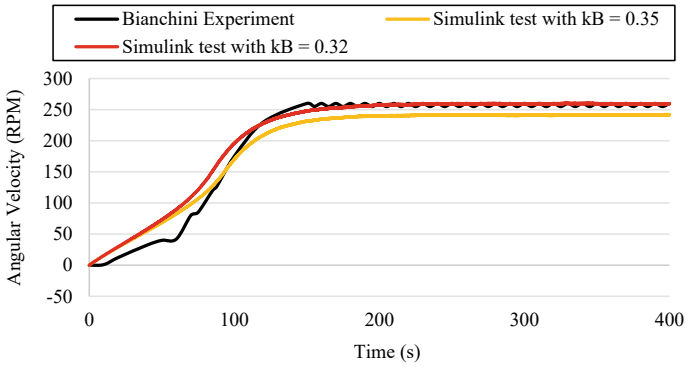

Fig. 4 Comparison between different kB of Simulink model test and Bianchini Experiment [31]

Model Gen has an influence on the maximum angular speed of the wind turbine. In addition, additional gain is also needed to match the wind turbine torque with the results of existing wind turbine research. Figure 3 illustrates the system that been found in this research. Coefficient A (kA) and the value of the coefficient B (kB) can be adjusted for generate a close enough result compared to another or real experiment test result.

Until the time of writing this paper, the nature of this coefficient had not yet been fully understood. A provisional hypothesis is that there may be a relationship between these two coefficients and the theory of momentum. This is because when using other wind turbine parameters, even with the same H-type and airfoil, the results do not match immediately with other resources such as real experiments or data from other journals. The calculation results only match when adjusting these two coefficients to fit at least one condition. For this study, $kA = 0.08$ and $kB = 0.35$ are used.

Figure 4 is a graph produced by the Simulink test and Bianchini experiment. There are three graphs, namely the model test with $kB = 0.35$ and 0.32. Of course, the kA used for both is the same. Two graphs produced by Simulink are compared with the graph from Bianchini's test, where he tested with the same VAWT parameters used in this experiment. When compared, the graph results closely approximate the graph obtained by Biancini, who used a Wind Tunnel Test to test his wind turbine. This comparison result shows that the model used for simulation in this paper is valid.

4 Research and Discussion

The research will be carried out by running a Simulink model that contains the previously determined parameters and discovered equation which it applied at the Simulink models with the end of the model to calculate angular velocity was shown in Fig. 2. The resulting data of angular velocity, C_p, and torque will be analyzed.

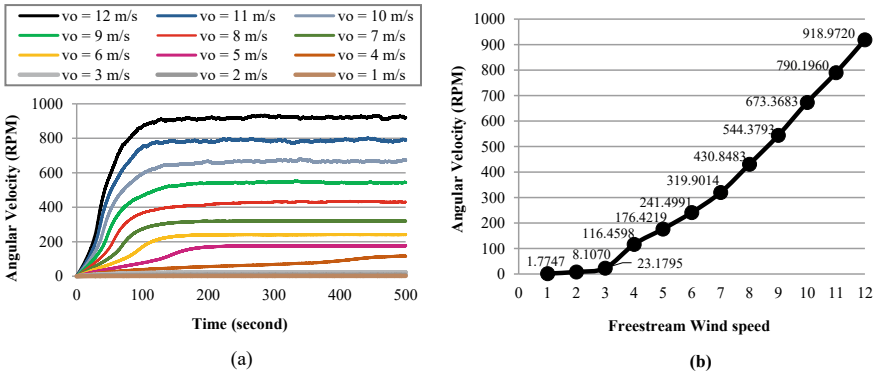

Fig. 5 **a** Angular velocity plot while turbine at start up condition. **b** Angular velocity at $t = 500$ s versus freestream wind speed [32]

The phenomenon of angular velocity will be observed while the wind turbine runs for 200 s with freestream wind speeds (Vo) ranging from 1 to 12 m/s.

Figure 5 depicts the relationship between Angular Velocity and wind speed. In Fig. 5a, it is evident that the turbine attains a steady state condition when the wind speed is at its maximum for every given speed. Although the angular velocity increases with wind speed, the time required to reach steady state is not always linear. However, the steady state time is always proportional to wind speed. Figure 5b illustrates that the angular velocity exhibits an almost linear trend with wind speed. The maximum angular velocity of 918.9720 rpm is observed at a wind speed of 12 m/s, while the minimum angular velocity of 1.7747 rpm is recorded at a wind speed of 1 m/s.

Certain aspects of wind turbine performance can be determined by analyzing the torque generated during rotation. Greater torque indicates that the turbine will have difficulty stopping. Figure 6 presents a plot of C_p and torque during the turbine's initial rotation until 200 s of operation. From the figure, it can be observed that both variables exhibit a common feature of rising and falling as if oscillating at a high frequency.

The simulation was carried out through multiple iterations until a total time of 500 s was reached. When plotting the torque and C_p values at the 200-s mark, the calculations was conducted for a total of 4689 iterations. Due to the high frequency of the torque and C_p values, a moving average of 50 iterations was employed to determine whether these variables tended towards a positive or negative trend.

Figure 6, shows that both have a peak value when the time is around 100 s. After that, the red line which is the moving average is decreasing. When $t = 120$ s, the moving average line no longer decreases and stays around the value torque and C_p equals to 0. This means that when the time shows 100 s, the value of the angular velocity is increasing and starting to enter a steady state. Only when the time shows 120 s, the steady state starts and the value of the angular velocity no longer increases.

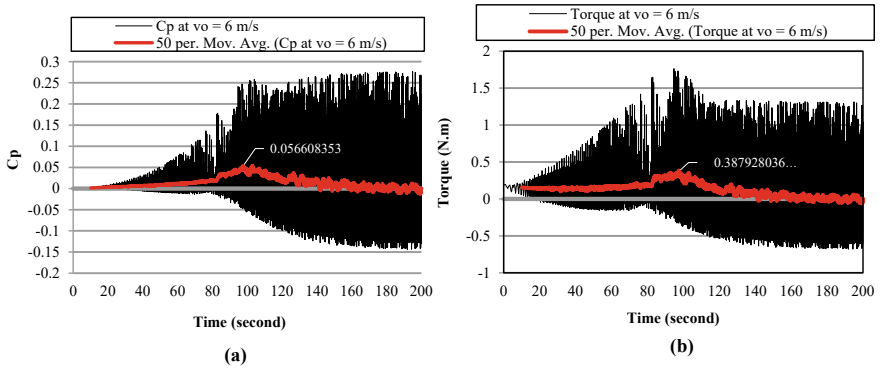

Fig. 6 **a** C_p and **b** torque plot during start-up ramp untill the angular velocity is steady [33]

To understand why the torque and C_p oscillate very quickly, the influence of the azimuth angle on torque and C_p was investigated. The experimental results are shown in Fig. 6, which illustrate the influence of the azimuthal angle on torque and C_p at times $t = 99$ s and $t = 199$ s. Referring to Fig. 5, the time $t = 99$ s is the peak of the moving average torque and C_p values, which represents the final start-up ramp condition. The torque test and C_p experiment were conducted at the end of 199 s, at which time the turbine was already in steady condition.

From Fig. 7, both (a) and (b), show us that the turbine will have a negative value of torque and C_p when the Azimuthal Angle is between 0 to 180 degrees, while the positive value is in the position of 180° to 360°. There are two points where the value of torque and C_p is 0, which is around 180° and 300°. The two 0 points where the three blade torques have positive and negative values, so they eliminate each other. Please note that the wind is blowing from 180° and moving to 360°.

Additionally, the torque and C_p values were examined as the freestream windspeed varied from 1 to 12 m/s. Although the experiment yielded a similar plot shape, the

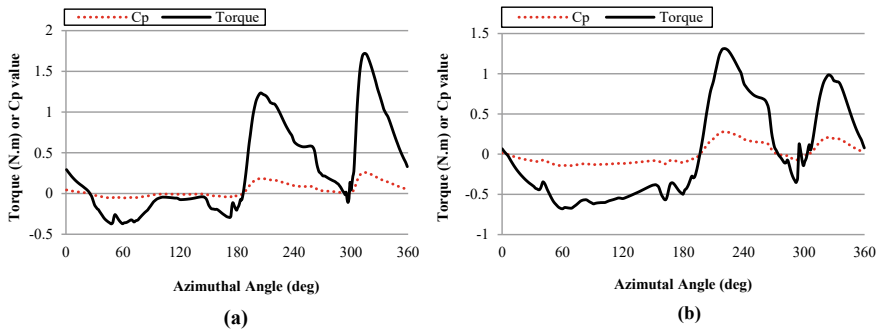

Fig. 7 C_p and torque versus Azimuthal angle at **a** final start-up ramp condition and **b** steady condition [34]

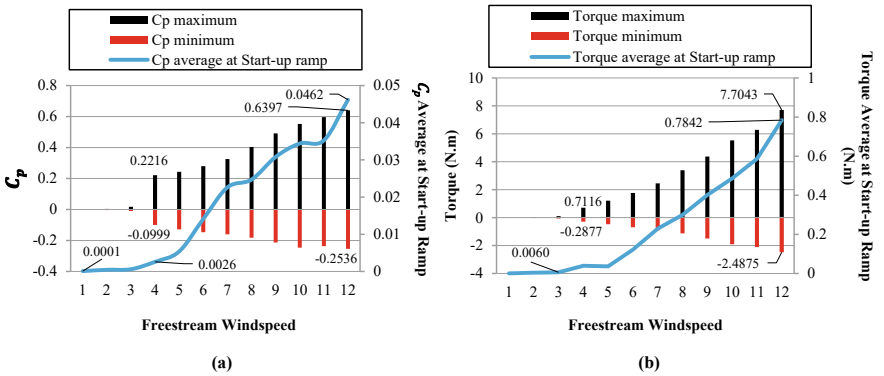

Fig. 8 **a** *Cp* and **b** Torque versus wind speed [33]

maximum and minimum values were different. Figure 8 displays the maximum and minimum torque values and C_p for various freestream windspeeds. To determine the actual performance of the wind turbine during rotation, an average value of the torque and C_p was calculated solely during the start-up ramp conditions.

Figure 8a depicts that the amplitude of torque and C_p plots is directly proportional to the freestream wind speed. At $vo = 12$ m/s, the C_p amplitude reaches its maximum value of 63.97%. However, the maximum C_p at average start-up ramp condition is only 4.6%. Figure 8b shows the amplitude values and average torque at start-up ramp conditions. The results indicate that during start-up in ramp conditions, the average torque has a maximum value of 0.78 N m. Both plots in Figure 8 illustrate that the torque and Cp values are significantly small when the vo values are between 1 and 3 m/s. It suggests that even the slightest disturbance can stop the turbine.

5 Conclusion

The performance of a Novel Simulink model shows that it can provide sufficiently accurate results when compared to Bianchini's experimental results. The VAWT with NACA 0015 airfoil has been evaluated using the model created, where some of the input parameters such as the number of blades, wind speed, radius, and chord length are used to produce outputs in the form of angular velocity and torque at start-up conditions, these results can be used to observe the phenomenon of wind turbine movement during start-up conditions. For further research, the created model can also be used for analyzing installed generator performance in the VAWT. According to the simulation results, the best operating condition for a VAWT is when the freestream wind speed is at 12 m/s, but it can still operate when the freestream wind speed is below 4. When the freestream wind speed is less than 4, it would be challenging for the VAWT to generate energy due to the slightest disturbance that can cause the turbine to stop as a result of the small torque acting on it. It is also observed that the

freestream wind speed has an influence on the speed of the turbine to reach a steady state.

This paper demonstrates that a low-speed wind turbine ($vo < 12$) can be operated with the NACA 0015 symmetrical airfoil. The analysis conducted using the Simulink model is just the first step towards a more in-depth analysis of wind turbines. However, further development and testing are necessary, especially in determining kA and kB in Dynamic Measurement. Without knowing kA and kB, data from other simulations or experiments from the actual device must be compared to determine them. This poses a challenge to the use of the model. If kA and kB can be determined, this model can potentially develop further to simulate all situations and conditions, including when the device is connected to the generator.

References

1. Pata UK (2021) Renewable and non-renewable energy consumption, economic complexity, CO_2 emissions, and ecological footprint in the USA: testing the EKC hypothesis with a structural break. Environ Sci Pollut Res 28(7):846–861
2. Mehmood I et al (2020) Carbon cycle in response to global warming. Environ Climate Plant Vegetation Growth 1–15
3. Al-Ghussain L (2019) Global warming: review on driving forces and mitigation. Environ Prog Sustain Energy 38(1):13–21
4. Perera FP (2017) Multiple threats to child health from fossil fuel combustion: impacts of air pollution and climate change. Environ Health Perspect 125(2):141–148
5. Iyer GC et al (2015) The contribution of Paris to limit global warming to 2 °C. Environ Res Lett 10(12):125002
6. Welsby D et al (2021) Unextractable fossil fuels in a 1.5 °C world. Nature 597(7875):230–234
7. Gielen D et al (2019) The role of renewable energy in the global energy transformation. Energ Strat Rev 24:38–50
8. Augusta FA et al (2020) Vertical axis wind turbine analysis using MATLAB. J Phys Conf Ser 1517(1):012065
9. Johari MK, Jalil M, Shariff MFM (2018) Comparison of horizontal axis wind turbine (HAWT) and vertical axis wind turbine (VAWT). Int J Eng Technol 7(4.13):74–80
10. Shah SR et al (2018) Design, modeling and economic performance of a vertical axis wind turbine. Energy Rep 4:619–623
11. Liew HF et al (2020) Review of feasibility wind turbine technologies for highways energy harvesting. J Phys Conf Ser 1432(1):012059
12. Brownstein ID, Wei NJ, Dabiri JO (2019) Aerodynamically interacting vertical-axis wind turbines: performance enhancement and three-dimensional flow. Energies 12(14):2724
13. Maleki Dastjerdi S et al (2021) Application of simultaneous symmetric and cambered airfoils in novel vertical axis wind turbines. Appl Sci 11(17):8011
14. Rogowski K, Hansen MOL, Bangga G (2020) Performance analysis of a H-Darrieus wind turbine for a series of 4-digit NACA airfoils. Energies 13(12):3196
15. Wang Y et al (2018) Investigation on aerodynamic performance of vertical axis wind turbine with different series airfoil shapes. Renew Energy 126:801–818
16. Song C et al (2020) Study on aerodynamic characteristics of darrieus vertical axis wind turbines with different airfoil maximum thicknesses through computational fluid dynamics. Arab J Sci Eng 45:689–698
17. Jang H et al (2021) Performance evaluation and validation of H-darrieus small vertical axis wind turbine. Int J Precision Eng Manuf Green Technol 1–11

18. Rodrigues G, Valério D, Melicio R (2022) Controller development and experimental validation for a vertical axis wind turbine. Sustainability 14(20):13498
19. Ranjbar MH et al (2019) Reaching the betz limit experimentally and numerically. Energy Equip Syst 7(3):271–278
20. Safarov A, Mamedov R (2021) Study of effective omni-directional vertical axis wind turbine for low speed regions. IIUM Eng J 22(2):149–160
21. Divakaran U et al (2021) Effect of helix angle on the performance of Helical Vertical axis wind turbine. Energies 14:393–417
22. Castillo J (2012) Small-scale vertical axis wind turbine design. Bachelor's thesis, Universitat Politècnica de Catalunya
23. Chabane F, Barkat MA, Arif A (2022) Aerodynamic shape optimization of a vertical-axis wind turbine with effect number of blades. DYNA: revista de la Facultad de Minas. Universidad Nacional de Colombia. Sede Medellín 89(220):154–162
24. Wang Z, Zhuang M (2017) Leading-edge serrations for performance improvement on a vertical-axis wind turbine at low tip-speed-ratios. Appl Energy 208:1184–1197
25. Chen Y, Lian Y (2015) Numerical investigation of vortex dynamics in an H-rotor vertical axis wind turbine. Eng Appl Comput Fluid Mech 9(1):21–32
26. Damon Woods L (2014) Simulation of VAWT and hydrokinetic turbines with variable pitch foils. Master's thesis, Boise State University
27. Manwell JF, McGowan JG, Roger AL (2009) Wind energy explained—theory,design, and application, 2nd edn. Willey, London, pp 147–148
28. Hasan A (2015) Model-based design and development of a vertical axis wind turbine computational model. Master's thesis, De Monfort University
29. Daowd M et al (2011) Passive and active battery balancing comparison based on MATLAB simulation. In: 2011 IEEE vehicle power and propulsion conference. IEEE, pp 1–7
30. Radha R (2022) Analysis of increase in average temperature on earth, its causes and wildfire using machine learning techniques. In: 2022 2nd Asian conference on innovation in technology (ASIANCON). IEEE, pp 1–13
31. Bianchini A, Ferrari L, Magnani S (2011) Start-up behavior of a three-bladed H-Darrieus VAWT: experimental and numerical analysis. In: Turbo expo: power for land, sea, and air, pp 811–820
32. Maalouly M et al (2022) Transient analysis of H-type vertical axis wind turbines using CFD. Energy Rep 8:4570–4588
33. Cai X et al (2020) Performance and effect of load mitigation of a trailing-edge flap in a large-scale offshore wind turbine. J Marine Sci Eng 8(2):72
34. Pucci M et al (2022) A DMST-based tool to establish the best aspect ratio, solidity and rotational speed for tidal turbines in real sea conditions. J Ocean Eng Marine Energy 8(3):285–303